Miscibility and Crystallization in Polycarbonate/Poly(ε-caprolactone) Blends: Application of the Self-Concentration Model

ARTICLE *in* MACROMOLECULES · MAY 2005

Impact Factor: 5.8 · DOI: 10.1021/ma050481c

7 AUTHORS, INCLUDING:

Dinorah Herrera de Newman
Simon Bolívar University
10 PUBLICATIONS **88** CITATIONS
SEE PROFILE

Alfredo Bello
Simon Bolívar University
90 PUBLICATIONS **799** CITATIONS
SEE PROFILE

Mario Grimau
46 PUBLICATIONS **493** CITATIONS
SEE PROFILE

Estrella Laredo
Simon Bolívar University
131 PUBLICATIONS **1,345** CITATIONS
SEE PROFILE

Miscibility and Crystallization in Polycarbonate/Poly(ϵ-caprolactone) Blends: Application of the Self-Concentration Model

Dinorah Herrera,[†] Jean-Carlos Zamora,[‡] Alfredo Bello,[†] Mario Grimau,[‡] Estrella Laredo,*[,†] Alejandro J. Müller,[‡] and Timothy P. Lodge[§]

Physics Department and Materials Science Department, Universidad Simón Bolívar, Apartado 89000, Caracas 1080-A, Venezuela, and Department of Chemistry and Department of Chemical Engineering & Materials Science, University of Minnesota, Minneapolis, Minnesota 55455-0431

Received March 7, 2005; Revised Manuscript Received April 22, 2005

ABSTRACT: Polycarbonate/poly(ϵ-caprolactone) (PC/PCL) blends are found to be miscible when extruded samples are studied without any further thermal treatment. PCL crystallizes in blends containing 60% or less polycarbonate, a component that remains amorphous for all blend compositions under these conditions. Single, broad calorimetric glass transitions together with distinct component dynamics determined by thermally stimulated depolarization current experiments indicate the miscibility of the blends and the existence of different average local compositions. The Lodge−McLeish model is applied to the compositional variation of the two effective glass transition temperatures. Quantitative agreement is obtained for both components by adjusting the self-concentration values to best fit the experimental points. The relevant length for PCL is very close to its Kuhn length, whereas for PC the best fit leads to a slightly shorter characteristic length. It is shown that upon annealing at sufficiently high-temperature PC undergoes crystallization and thereby induces phase segregation in the otherwise amorphous regions of the blends.

1. Introduction

Mixtures of bisphenol A polycarbonate (PC) and poly(ϵ-caprolactone) (PCL) have been extensively studied, and many apparently conflicting results have been obtained on this system, to the point that it has been labeled the "Gordian blend system" by Varnell et al.[1] The blends have been regarded by many authors as fully miscible on account of the finding of one calorimetric glass transition temperature, T_g, that varies with composition within a range encompassed by the T_g's of the pure components.[2−8] However, the temperature range for the T_g calorimetric step in the blends is broader than in the neat components, and this broadening is nonsymmetric with composition. In a preceding work on this system,[9] we demonstrated that blends that had been stored at room temperature for 18 months and that were originally regarded as miscible[8] (since they had exhibited a single T_g as determined by differential scanning calorimetry, DSC) were now either partially mixed or phase separated, depending on their thermal treatment. Phase separation was demonstrated by DSC, transmission electron microscopy, spherulitic growth rate measurements, and thermally stimulated depolarization currents (TSDC). The driving force behind phase segregation was attributed to the slow PCL crystallization during storage. The only way to restore miscibility in these phase-separated blends was to subject them to extrusion or dissolution and reprecipitation.

This particular system is interesting in that both components may crystallize. Consequently, at any temperature the blend might form an amorphous, one-phase mixture or undergo liquid−liquid phase separation. Below the crystallization temperature of PC (ca. 230 °C) or PCL (ca. 60 °C) crystallization of either (or both) components could occur, leading to two or three coexisting phases, with interfacial zones of varying composition. Furthermore, the glass transitions of the components are extremely widely separated (140 °C for PC, −66 °C for PCL). Both the structure and the dynamics in such a system are expected to be quite rich and thermal history dependent.

In a miscible blend, in addition to the intermediate and broad calorimetric glass transition, distinct component dynamics have often been found. This "dynamic heterogeneity" has been widely studied, and several explanations have been proposed. One approach is that the local concentration variations result from the effect of thermal concentration fluctuations.[10−12] Another approach by Lodge and McLeish[13] emphasizes chain connectivity effects or "self-concentration", which result in effective glass transitions for each component, $T_g^{eff}(\phi)$, based on the average local composition perceived by each component. These may be quite different from that of the bulk composition. Various experiments, such as dielectric spectroscopy if the two blend components are polar, are able to distinguish different dynamics, i.e., different $T_g^{eff}(\phi)$ for each component, in agreement with the dynamic heterogeneity explained by the self-concentration model. The model is able to rationalize the compositional variations of the $T_g^{eff}(\phi)$'s. The original calculations were based on the Kuhn segment length, l_K, as the relevant length scale for the self-concentration application. Once the self-concentrations ϕ_{SA} and ϕ_{SB} are calculated from the volume fraction occupied by a Kuhn length's worth of monomer within a volume $V \sim l_K^3$, the effective local concentration is estimated for each component, ϕ_{effA} and ϕ_{effB}. The Fox equation is then used with the effective concentrations to calculate the effective glass transition temperatures for components A and B, $T_{gA}^{eff}(\phi)$ and $T_{gB}^{eff}(\phi)$. One important consequence of this approach is that a fully miscible, molecularly mixed blend can still exhibit two

[†] Physics Department, Universidad Simón Bolívar.
[‡] Materials Science Department, Universidad Simón Bolívar.
[§] University of Minnesota.
* Corresponding author. E-mail elaredo@usb.ve.

10.1021/ma050481c CCC: $30.25
Published on Web 05/18/2005

glass transitions; there is no need to invoke large scale spatial "heterogeneities" or "partial miscibility" to explain this observation.

The model has been initially tested for several blend systems whose dynamics had been followed by, e.g., tracer diffusivities and nuclear magnetic resonance spectroscopy (NMR).[13] Segmental dynamics observed by dielectric spectroscopy in several miscible blends have also been used to test the model.[14] In this latter work, the self-concentration is not estimated from the Kuhn length but results from the fit of experimental points to the Fox equation, which enables the calculation of the blend effective T_g values from the fitted ϕ_{eff}. More recently, the model has been tested on other blend systems such as polystyrene/poly(vinyl methyl ether), PS/PVME, polystyrene/poly(*o*-chlorostyrene), PS/PoClS, and PVME/PoClS,[15] and its quantitative predictions agree well with the TSDC results if the Brekner equation[16] is used to fit the T_g compositional variation obtained by DSC. Other applications of the model published in the past 2 years are available, in systems such as polyisoprene/poly(vinyl ether), PI/PVE, thoroughly studied by NMR, rheology, and dielectric spectroscopy.[17] The PI results agree well with the predictions of the model over the composition and temperature range explored, while for PVE the agreement is somewhat less satisfactory. It should be noted that the self-concentration model, which is appealing for its simple assumptions, has not been applied to blend systems where both components are crystallizable and polar.

In the present work, we reexamine PC/PCL blends prepared in such a way that by calorimetric techniques they exhibit a single T_g over the composition range. DSC, wide-angle X-ray scattering (WAXS), TSDC, and dynamic mechanical thermal analysis (DMA) experiments are combined to follow the behavior over wide temperature and concentration ranges. The variety of techniques probe the material at different scales as TSDC resolves distinct $T_g^{eff}(\phi)$'s for the two dielectrically active components while DSC responds to the bulk average T_g. Because of the simplicity and demonstrated ability of the Lodge and McLeish model, it has been used to interpret our experimental results so as to shed light on the physics behind the remarkable plasticization effect that PCL induces in PC. Finally, the effect of crystallinity on the blend miscibility is studied by isothermally crystallizing the PC component; in the presence of crystalline PC the phase separation is demonstrated by the development of a PCL amorphous phase that is almost pure and that is clearly detected by DSC.

2. Experimental Section

2.1. Materials. A bisphenol A polycarbonate (PC) manufactured by Bayer, Makrolon 2807, with a molecular weight, M_w= 30 000 g/mol, and an ϵ-polycaprolactone (PCL), TONE P787, manufactured by Union Carbide Corp., with a M_w = 120 000 g/mol were employed. Size exclusion chromatography experiments employing polystyrene calibration standards yielded values of M_w = 131 000 g/mol and M_w/M_n = 1.47 for PCL and M_w = 32 000 g/mol and M_w/M_n = 1.95 for PC.

To prepare melt-extruded blends, we first dried the PC in a vacuum oven at 100 °C for 4 days. The mixing was performed with a laboratory scale extruder (Atlas 1820) at 190−210 °C in the die and 230−260 °C in the barrel zone, depending on blend composition. A film die was employed to obtain thin ribbons of about 9 mm width and 0.3 mm thickness. The ribbons were air-cooled as they left the die. The global compositions studied here vary from pure PC, 100/0 blend, to pure PCL, 0/100, in 10% increments.

2.2. Wide-Angle X-ray Scattering. The WAXS experiments were carried out with an automatic Philips diffractometer at room temperature, by using an acceleration voltage of 40 kV and a current of 40 mA. The Ni-filtered Cu Kα wavelength was used. The scans were made from 5° to 40 ° in 2θ by 0.020° steps at a sweep rate of 0.01°/s. The samples were cut from the same extruded strips that were used for the parallel experiments. The weight fraction crystallinity degree, X_c, determination was performed by decomposing the spectrum with the Peakfit commercial software. The experimental trace is made by the Gaussian amorphous halos corresponding to the amorphous fraction of both the PC and the PCL in addition to the Bragg reflections given by the PCL crystal lamellae which have a nonplanar orthorhombic structure with space group $P2_12_12_1$.[18] The profile of the PC amorphous phase is known from neat PC spectrum and the PCL halo from the molten PCL spectrum. No trace of the presence of the monoclinic crystalline PC was detected in the whole composition range on as-extruded samples.

2.3. Differential Scanning Calorimetry (DSC). The calorimetric behavior of the samples was obtained with a Thermal Analysis, TA DQ100, DSC instrument with a liquid-nitrogen cooling system. The instrument was calibrated with indium, and helium purge gas was employed. The sample weights were 14−15 mg, and they were encapsulated in aluminum pans. Standard DSC scans were recorded at 20 °C/min from −80 to 250 °C. Isothermal crystallization experiments were also performed, in which each sample was heated to 250 °C and held at that temperature for 3 min. Then, the sample was quenched (60 °C/min) to a selected crystallization temperature, T_c, and held at that temperature during a specific crystallization time, t_c. Then a cooling scan was recorded (at 20 °C/min) down to −80 °C. Finally, a heating scan from −80 to 250 °C was recorded at 20 °C/min to examine the melting behavior.

2.4. Thermally Stimulated Depolarization Current (TSDC). The cryostat of the fully automated TSDC measuring system has been designed in our laboratory. The sample is located between two parallel stainless steel plates, which are connected to the high-voltage supply during the polarization step by means of thin-wall stainless tubing in order to avoid losses by heat conduction. After the polarization of the sample at the chosen polarization temperature T_p, the polarization is frozen-in by quenching the sample to liquid nitrogen temperature. After allowing time to discharge any mobile charges, the sample is heated with a constant heating rate of b_h = 0.07 °C/s. The depolarization current density caused by the return to equilibrium of the previously oriented dipoles is recorded with a Keithley 642 electrometer. The current density peaks caused by the polarization decay due to each type of dipole occur at temperatures where the relaxation time of the dipolar species reaches the time scale of the experiment. The equivalent frequency for this dielectric experiment is estimated to be about 30 mHz. This low equivalent frequency results in a very good resolution for this technique. Another important advantage is the peak separation that can be performed by choosing adequately the polarization temperature and partially depolarizing the sample during the heating. All the TSDC curves presented here have been normalized to a polarizing field of 10^7 V/m, an area of 10^{-4} m^2, and a thickness of 100 μm.

2.5. Dynamic Mechanical Analysis (DMA). A Rheometrics RSA-II instrument was employed. The chosen test was dynamic longitudinal tension at 1 Hz, the heating rate was 2 °C/min in a temperature range between −80 and 160 °C, and the strain was fixed at 0.5%.

3. Results and Discussion

3.1. WAXS Results. The results of the WAXS experiments performed at room temperature on the extruded blend ribbons are plotted in Figure 1 as a function of the diffraction angle, 2θ, for blends over the whole

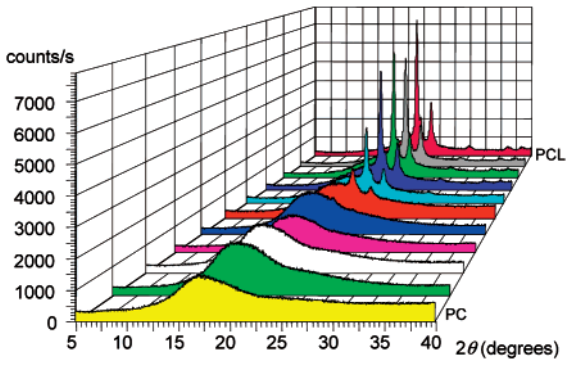

Figure 1. WAXS spectra of the PC/PCL blends with Cu Kα radiation. The bulk PCL concentration increases by 10% steps on going from front (PC) to back (PCL).

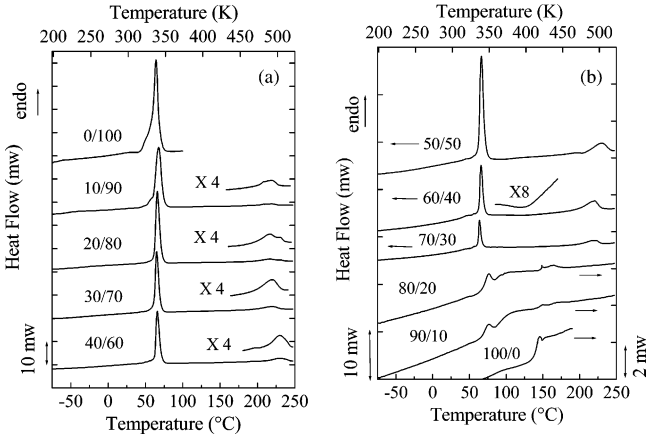

Figure 2. DSC first heating scans (20 °C/min) of PC/PCL extruded blends: (a) PCL and PCL rich blends; (b) PC and PC rich blends. The global compositions are indicated above the traces.

composition range. It is clearly observed that for the PC-rich blends the material is 100% amorphous. As the mid-composition range is reached, the Bragg peaks of PCL, which were barely visible for the 40/60 PC/PCL blend, start to increase, ultimately leading to a crystallinity degree of 55% for the pure PCL homopolymer. No trace of crystallization of the PC component was detected throughout the whole concentration range. This is a different result as compared to our previous work on this same blend system,[9] where in the compression-molded samples crystallites of both PC and PCL coexisted in samples rich in PCL. Interestingly, in that case the formation of PC crystallites in the blends could be induced by isothermal crystallization on a time scale much shorter than that required for pure PC. For example, in the case of a 90/10 blend PC crystallinity values of 17% were reached in less than 8 h at 145 °C,[19] demonstrating the plasticization effect of PCL on PC. From the WAXS traces obtained here the crystallinity degrees at room temperature were calculated by a deconvolution process of the PC/PCL amorphous contribution, in addition to the crystalline Bragg reflections of PCL. The crystallinity degrees of the PCL component in the blends were 0.5% for 70/30, 21.2% for 50/50, 42.6% for 30/70, 58.6% for 10/90, and 55.1% for the neat PCL. Compositions of the amorphous phase were recalculated by taking into account the corresponding crystalline content in each sample. The corrected values for the PC concentration in the amorphous phase will be used in subsequent figures and labeled as ϕ_{Bcorr}.

3.2. DSC Results. DSC heating scans of extruded blends, which were first cooled from room temperature to −75 °C, are shown in Figure 2a,b. The WAXS results of Figure 1 demonstrated that only the PCL component was able to crystallize during the air cooling process applied at the extruder exit in the case of the PCL rich blends, while the PC remained amorphous for all blend compositions examined. Nevertheless, during the heating scan in the DSC (Figure 2a,b), the PC component is capable of undergoing cold crystallization (and therefore phase segregation) as the melting endotherms near 230 °C corresponding to the PC crystals formed during the heating scan indicate. The exotherms corresponding to cold crystallization are rather difficult to see since they are very broad and could be masked by the baseline. In the case of the 60/40 PC/PCL blend in Figure 2b the cold crystallization of PC can be observed in the magnified section above the corresponding DSC trace; a similar behavior has been previously reported before.[8] The PCL component was also able to crystallize during the heating scan and cold crystallization exotherms can be seen for some blend compositions when a close-up of the scan is examined. (The scale employed in Figure 2 does not allow the observation of such broad and small cold crystallization exotherms.)

Evidence that the PCL component has crystallized during the heating scan is provided in Figure 2b since melting endotherms corresponding to PCL are observed over the entire composition range, while WAXS performed at room temperature clearly showed that no PCL crystals were present in PC-rich blends. Nevertheless, the endothermic peaks located at typical PCL component melting temperatures near 70 °C for the 80/20 and 90/10 PC/PCL blends are small and in a temperature range that overlaps with the T_g of the amorphous phase of the blend. Therefore, they may also be entwined with enthalpy-relaxation phenomena due to the molecular orientation imparted during extrusion. The ability of the PC and the PCL to undergo cold crystallization is probably enhanced by chain orientation induced during the extrusion process. If this is the case, a second heating run after erasing the thermal history should show differences with respect to the first heating scan, as will be demonstrated below.

Figure 3a,b shows cooling scans after annealing at 250 °C for 3 min. The characteristic variation in C_p at T_g can be observed over the entire composition range, and it is evident that the region where the single glass transition occurs shifts to higher temperatures with the addition of the higher T_g component. The PC component was not able to crystallize during the cooling scan, while the PCL did crystallize in the 30/70, 20/80, and 10/90 PC/PCL blends. These DSC cooling scans indicate that the blends are miscible in the liquid and glassy states, as can be inferred by the presence of a single calorimetric T_g.

It is interesting to compare the width of the C_p step associated with the vitrification process of the homopolymers and the blends in Figure 3. The PC homopolymer exhibits a relatively narrow C_p change as it goes from the rubber to the glass state. In contrast, the PC-rich blends display very broad T_g regions. The width of the transition apparently increases with PCL content from 0 up to 40%. Then at 50% or higher PCL content the T_g region narrows once more. For instance, if a comparison is made between the width of the T_g corresponding to the 60/40 PC/PCL blend and the 40/60 blend, it is evident that the blend with a higher PC

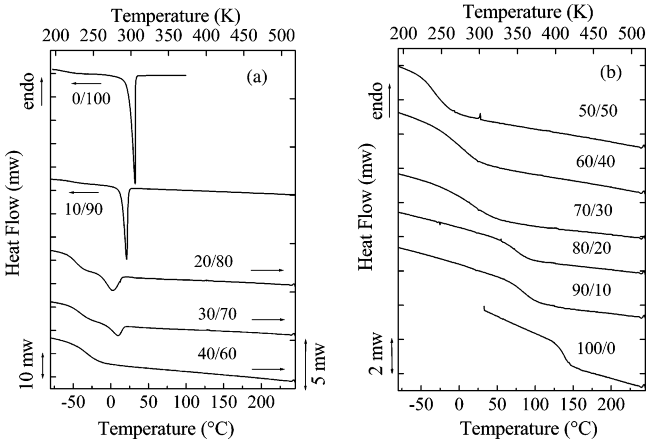

Figure 3. DSC cooling scans (20 °C/min) of PC/PCL blends. The samples were first heated to 250 °C (as shown in Figure 1) and annealed at that temperature for 3 min before recording the cooling scans. (a) PCL and PCL rich blends; (b) PC and PC rich blends. The global compositions are indicated above the traces.

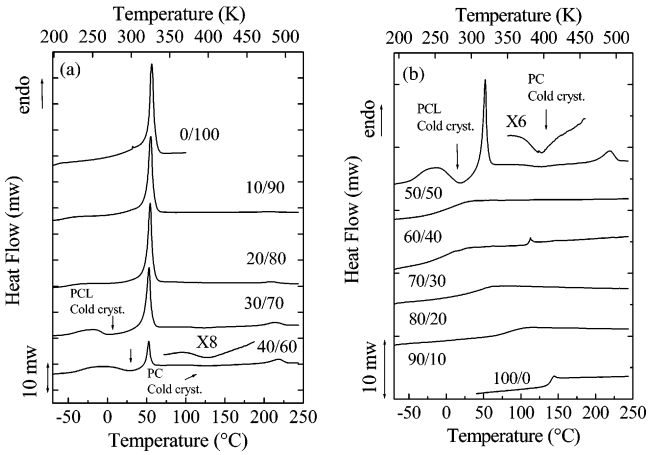

Figure 4. DSC second heating scans (20 °C/min) of PC/PCL blends. The scans were recorded immediately after the cooling runs performed in Figure 2. (a) PCL and PCL rich blends; (b) PC and PC rich blends. The global compositions are indicated above the traces.

content displays a broader transition. This nonsymmetric broadening of the calorimetric T_g in miscible blends has been predicted by the model of Lodge and McLeish.[13] According to this model, the lower T_g blend component (i.e., PCL) will show segmental dynamics nearer to that of the homopolymer, whereas the segmental dynamics of the higher T_g component will be closer to the blend average. The width of the transition is smaller for blends richer in the higher T_g component, as the slope of the underlying $T_g(\phi)$ is greater in this region.

Figure 4 shows the second DSC heating scans, performed immediately after the cooling scans shown in Figure 3. As in the first scan (Figure 2), it is possible to see melting endotherms for the PC component, although PC was not able to crystallize during the cooling scans shown in Figure 3. This is another confirmation of the ability of the PC component to experience cold crystallization during the heating scan when it is mixed with PCL. A similar result is observed for the PCL component, since for the 50/50 and 40/60 PC/PCL blends the PCL component was not able to crystallize during the cooling scan (Figure 3), but it was able to do so during the heating scan in a rather evident cold crystallization process (Figure 4). The cold crystallization of both PC and PCL components for the 50/50 blend can be clearly observed in Figure 4b and are indicated with arrows. As in the cooling scans of Figure 3, the glass transition of the blends in the entire composition range can also be observed in Figure 4. An interesting result shown in Figure 4 is that there is no melting corresponding to the PCL component for the 60/40 and 70/30 PC/PCL blends, whereas in Figure 2 the PCL components in the same extruded blends exhibited clear melting endotherms. This is probably a consequence of the molecular orientation in the samples during the extrusion process; this orientation can facilitate nucleation leading to crystallization during the air cooling applied at the extruder exit. However, once the thermal history and orientation is erased, then only in blends with 50% PCL or more is the PCL component able to crystallize (either during cooling from the melt and/or during the heating scan, depending on composition).

The DSC results presented in this section have shown that: (1) The blends are found to be homogeneous in the bulk. (2) Depending on the composition, PC and PCL could crystallize during cooling from the melt and/or during the heating scan. PCL and PC do not cocrystallize; therefore, when they crystallize, they must phase separate from each other. (3) The blends are a complex system where subtle changes in composition, orientation, or thermal history can trigger nucleation and crystallization of either one or both components. Therefore, the system can experience a transition from one phase (all amorphous or molten PC/PCL blend) to a two-phase or even a three-phase system.

3.3. TSDC Results. Once the miscibility of the PC/PCL blends has been demonstrated by DSC, TSDC studies were performed to follow the molecular dynamics of the blend components. In the temperature range where the TSDC runs were performed no significant changes in crystallinities are expected, as can be seen in Figure 2a,b. The crystallinity degrees estimated from the WAXS experiments on the extruded strips are then used to calculate the corrected composition values of the blends. Several features are common in the spectra from the blends: (a) the low-temperature part of the spectrum from −193 to −93 °C is a broad band which is made of at least two relaxation modes, γ and β; (b) in the region from −73 up to 125 °C there are two distinct component dynamics. The higher temperature one, denoted α_B, is the dielectric manifestation of the glass transition of the PCL and PC chains in a cooperative volume strongly affected by connectivity effects. The maximum intensity of this peak is at least 10 times stronger than for the γ and β peaks, and the peak position varies from −67 to 119 °C as the PC fraction increases from 0 up to 100%. (c) For PC contents $\phi_B \geq 30\%$, on the lower temperature side of the α_B peak a broad and weak relaxation is present at temperatures somewhat higher than that of the α mode of the PCL homopolymer. It is located at 6 °C for the 90/10 PC/PCL blend and at −23 °C for the 50/50 blend; it will be labeled as the α_A mode.

The low-temperature spectra of the PC/PCL blends studied here are represented in Figure 5 for seven blend compositions. The two extruded homopolymers give very different intensities in this zone, the PC spectrum being very weak and flat. In a previous work the low-temperature spectrum of neat PC from a different manufacturer showed a rich structure which varied with

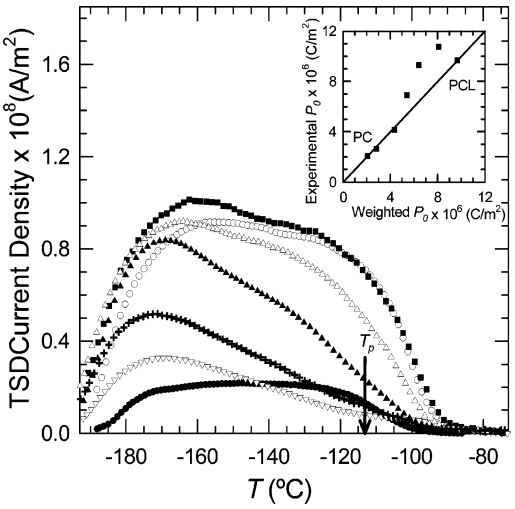

Figure 5. Low-temperature TSDC spectra of the extruded PC/PCL blends with bulk compositions: (●) 100/0; (▽) 90/10; (+) 70/30; (▲) 50/50; (△)30/70; (■) 10/90; (○) 0/100. The variation of the total measured polarization as a function of the weighted one is plotted in the inset, a 1 slope line is drawn.

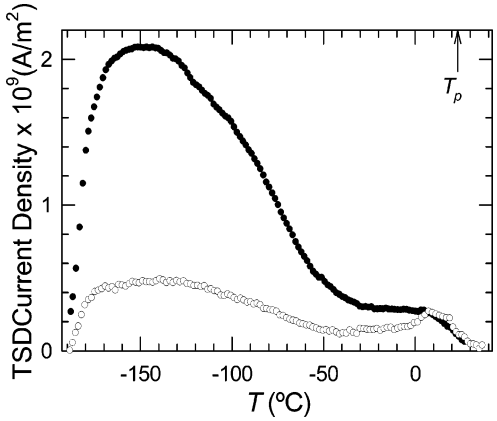

Figure 6. Low-temperature spectra of neat PC: (○) extruded sample; (●) molded samples at 240 °C from extruded strips.

the PC crystallization in acetone vapor.[20] Two distinct main modes, γ and β, were identified with increasing temperature, whose relative intensities change with the increasing PC crystallinity degree. The overall intensity of the low temperature spectrum decreased more rapidly than the loss of amorphous chains transferred to the crystalline regions as the PC crystallinity increases. The localized motions were affected by constraints applied to the PC amorphous regions either by the crystalline lamellae or by a rigid amorphous phase whose existence was demonstrated in the PC homopolymer. In the present work, the lack of structure observed in the low-temperature TSDC spectrum given by the extruded PC is compared in Figure 6 to that of a molded film made from the extruded ribbons. The important intensity differences are attributed to the preferential orientation of the chains in the extruded film that are sufficient to inhibit the localized motions of the polar groups of the PC amorphous chains.

For the PCL homopolymer, the γ and β relaxations have been extensively studied by dielectric spectroscopy,[21] and the main characteristics of these modes are the following: (a) the γ mode is more intense in dry samples and as the moisture content increases the β mode predominates; (b) their position and profile are not sensitive to the molecular weight; (c) there exists in neat PCL a merging of the α and β modes at high temperatures and low frequencies and a second merging at still higher temperatures of the $\alpha\beta$ and γ modes.

The effect of blending on the low-temperature modes has been studied by Katana et al.[22] for the tetramethylbisphenol A polycarbonate and bisphenol A polycarbonate, TMPC/PC, miscible mixtures. They report a linear variation of the dielectric strength of the β relaxation of each component with composition even though a selective inhibition of the local motions in PC is proposed to explain the shifts in temperature upon blending. In the case of the poly(4-vinylphenol)/poly(methyl methacrylate) the same linear increase with PMMA concentration for the β mode is observed, and it is concluded that blending does not affect the local β mode.[23]

As PC is added to PCL, the intensity and profile of the low-temperature spectrum change. It should be noted that the low-temperature spectra profile of the two homopolymers are composed of at least two modes and occur in the same temperature range, as both of them originate from short-range motions of the carbonyl group. Because of this overlap, it is difficult to follow the changes introduced by the blending on each component relaxations. However, one can observe that the overall intensity decreases with added PC, and the γ peak is now predominant over the β peak. For the PC-rich blends the addition of only 10% PCL is enough to change the position in temperature of this peak, showing that blending somewhat releases constrains on the short-range motions of the PC chains. At mid-compositions the γ peak is still predominant over the β peak, whose maximum is now coincident with that of the β peak of neat PCL. The effect of blending on the intensity of the low-temperature peaks, i.e., on the number of orientable dipoles, can be estimated by evaluating the area under the curves. The total polarization, $P_{0\mathrm{exp}}$, which is plotted in the inset of Figure 5, is calculated by the area under each curve of the current density plots, $J(T)$, times the heating rate. The abscissa, $P_{0\mathrm{weighted}}$, is evaluated by adding the contribution of each component according to the corrected blend composition. The points corresponding to the PC-rich blends are on the slope one line, but the experimental points for PCL-rich blends deviate from this behavior. One might speculate that this increase in the number of orientable dipoles in the PCL-rich blends could be attributed to the disappearance of constrains present in the amorphous phase. A high PCL concentration seems to be necessary in order to render mobile the whole PC blend component. At low PCL concentrations, this PC rigid amorphous phase do not contribute to the short-range motions of the macromolecular chain. This interpretation supports our previous findings about the existence of a rigid amorphous phase in neat PC.[20]

At higher temperatures the cooperative mobility becomes apparent. The α relaxation mode is the dielectric manifestation of the dynamic glass transition. For the two homopolymers the very well-defined α peaks are located at $T_{\mathrm{M}\alpha\mathrm{A}} = -67.6$ °C for the A component (PCL) with the lowest T_g and $T_{\mathrm{M}\alpha\mathrm{B}} = 118.4$ °C for the B component (PC). The normalized curves $J(T)/J_{\max}(T)$ are plotted for all concentrations in Figure 7, where in addition to an intense and well-defined mode at intermediate temperatures, a broad and weak peak on the low-temperature side of the intense peak is clearly visible. These two cooperative mobilities are interpreted

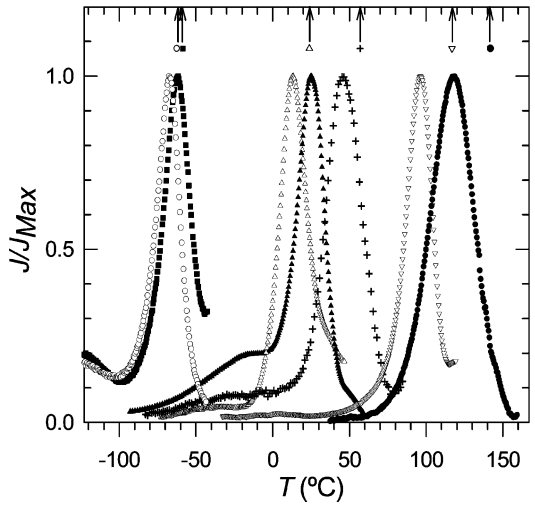

Figure 7. Segmental modes in PC/PCL blends with bulk compositions: (●) 100/0; (▽) 90/10; (+) 70/30; (▲) 50/50; (△) 30/70; (■) 10/90; (○) 0/100. Polarization temperatures are shown by arrows.

as the high and low effective T_g's that are predicted by the Lodge and McLeish model. The low-temperature segmental mode which corresponds to the local heterogeneities felt by PCL chains is a broad peak resulting from a wide relaxation time distribution as predicted by the model. The determination of T_{gA}^{eff} is not very precise even at this low equivalent frequency; however, it is a better estimation than the overlap that is observed by dielectric spectroscopy at higher frequencies between the two effective T_g's. By this latter technique, the existence of dynamic fluctuations is evidenced by an anomalous broadening of the α relaxation in the blends. These two distinct dynamic behaviors added to the unusually broad enthalpic steps observed in the DSC traces point to the existence of dynamic heterogeneity in the miscible system under study.

The Lodge and McLeish model[13] for miscible polymer blends calculates effective glass transitions based on the average local composition perceived by each component which may be quite different from that of the bulk composition. A first attempt to apply the Lodge and McLeish model to calculate the self-concentrations was performed by using the Kuhn segment lengths.

Additionally, the Fox equation was assumed to be an adequate description of the variation of the bulk T_g with composition, even though as can be seen in Figure 8, the experimental bulk T_g's as determined by DSC (symbols) did not follow the Fox equation (continuous line). Alternatively, the fit to Brekner's equation of the measured calorimetric T_g was used. The values of the characteristic ratio C_∞ used here to calculate the PCL Kuhn lengths were taken from Huang et al.[24] and Jones et al.[25] The first values were chosen as they are more recent and lead to more consistent results, $l_{KA} = 7.0$ Å. For PC the use of the values given by Fetters et al.[26] gave $l_{KB} = 15.7$ Å. The self-concentrations are then estimated through the equation

$$\phi_s = \frac{C_\infty M_0}{k\rho N_0 {l_K}^3} \tag{1}$$

Here M_0 is the repeat unit molar mass, k is the number of main chain bonds per repeat unit, ρ is the polymer density, and N_0 is Avogadro's number. The resulting self-concentration values are $\phi_{sA} = 0.33$ and $\phi_{sB} = 0.05$.

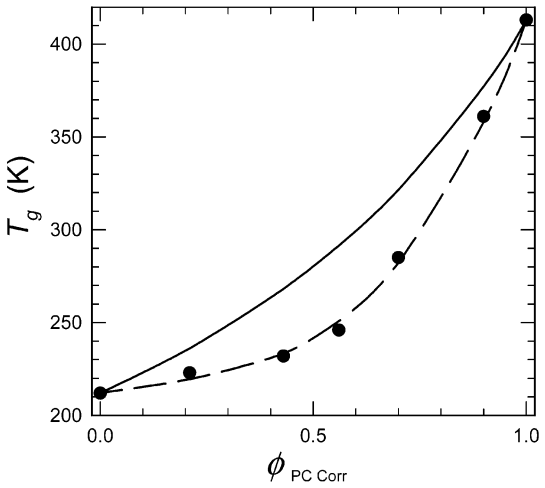

Figure 8. Calorimetric glass transition temperatures as determined by DSC (●) (first cooling): (– –) adjusted with Brekner equation ($k_1 = -0.7553$, $k_2 = 1.278$); (—) calculated with Fox equation.

Then, T_{gA}^{eff} and T_{gB}^{eff} were calculated by using the Fox equation

$$T_{gA}^{eff} = \left(\frac{\phi_{effA}}{T_{gA}} + \frac{1 - \phi_{effA}}{T_{gB}}\right)^{-1} \tag{2}$$

with the effective concentrations being

$$\phi_{eff} = \phi_s + (1 - \phi_s)\phi \tag{3}$$

The application of the model by using the estimated Kuhn lengths and the Fox equation leads to T_g^{eff} values which do not agree well with the TSDC determinations (symbols), as can be seen in Figure 9a (dotted and dashed lines). The low self-concentration value found for PC predicts that the T_{gB}^{eff} would be close to the average dynamics of the blend, i.e., close to the compositional dependence described by Fox equation (continuous line). This does not agree with the experimental determinations where the effective glass transition temperatures for the higher T_g component are quite distant from the predicted ones calculated by using $\phi_{sB} = 0.05$. The agreement is somewhat better for PCL than for PC.

A second attempt was made by adjusting the calorimetric glass transition temperature compositional dependence to the Brekner equation which has been widely used to describe this dependence:[15,16]

$$T_g(\phi_B) = T_{gA} + (T_{gB} - T_{gA})[(1 + k_1)\phi_B - (k_1 + k_2){\phi_B}^2 + k_2{\phi_B}^3] \tag{4}$$

The parameters k_1 and k_2 which characterize this cubic equation result from the fit of the experimental T_g's values as determined by DSC for various values of the crystallinity corrected bulk concentration of component B, which in our case is PC. It was found that the best fit represented in Figure 8 (interrupted line) is obtained for $k_1 = -0.7753$ and $k_2 = 1.278$. By using then the self-concentration values found above, i.e., the ones deduced from the Kuhn lengths, the effective local concentration is calculated for both components, assuming that the variation of both effective glass transition temperatures, follow the Brekner dependence with unchanged k_1 and k_2; $T_{gA}^{eff}(\phi) = T_{gA}(\phi_{effA})$ and $T_{gB}^{eff}(\phi) = T_{gB}(\phi_{effB})$ were

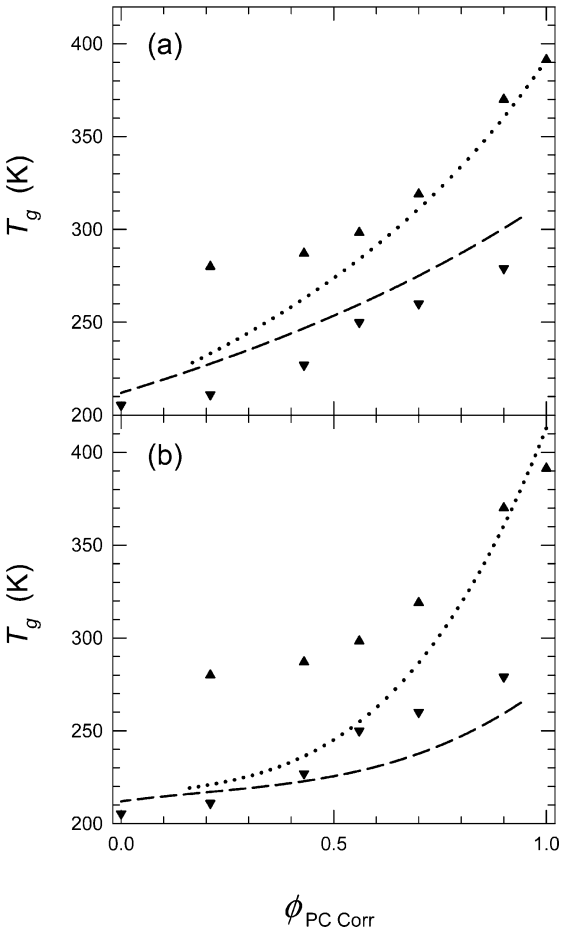

Figure 9. TSDC values for T_{gA}^{eff} (▼) and T_{gB}^{eff} (▲). Lines result from using the Kuhn's length to calculate the self-concentrations, i.e., $\phi_{sA} = 0.33$, $\phi_{sB} = 0.05$: (a) with Fox equation: T_{gA}^{eff} (− −), T_{gB}^{eff} (···); (b) with Brekner equation ($k_1 = -0.7553$, $k_2 = 1.278$): T_{gA}^{eff} (− −), T_{gB}^{eff} (···).

calculated. The resulting values are plotted in Figure 9b with dotted lines for the $T_{gB}^{eff}(\phi)$ and dashed line for $T_{gA}^{eff}(\phi)$. The agreement with the experimental determinations of the high and low T_g's is acceptable for the effective glass transition of the PCL chains but is definitely not satisfactory for the effective glass transition of the PC chains at high PCL concentrations; the calculated ϕ_{sB} value is too low to describe the differences between the average bulk T_g (continuous lines) and the effective $T_{gB}^{eff}(\phi)$ for PC chains. The conclusion of the different trials (Fox and Brekner) performed here to fit our TSDC results by using the estimated Kuhn lengths are barely acceptable for PCL but only present a qualitative agreement for the high effective temperature component, $T_{gB}^{eff}(\phi)$. In the application of the model to PI/PVE blend studied by NMR,[27] a similar situation was found, i.e., a quantitative agreement for the PI component with the higher self-concentration ($\phi_{sA} = 0.47$) and a qualitative agreement only for PVE ($\phi_{sB} = 0.25$).[17]

Following He et al.,[14] a series of fittings were performed where, instead of using the Kuhn length to evaluate the self-concentration, this parameter was fitted to the Lodge−McLeish model by using the Fox equation. $\phi_{sA} = 0.47$ and $\phi_{sB} = 0.19$ are now the fitted values for the self-concentrations. Characteristic lengths l_c can be calculated from these self-concentrations with eq 1, and these values are $l_{cA} = 6.2$ Å and $l_{cB} = 11.9$ Å. The PCL characteristic length is close to l_{KA} while for

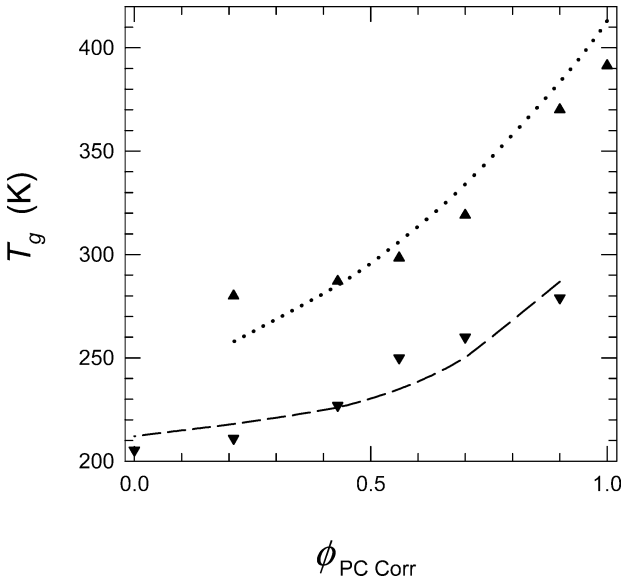

Figure 10. TSDC values for T_{gA}^{eff} (▼) and T_{gB}^{eff} (▲). The lines are the fit to the Brekner equation, and the adjusted self-concentrations are $\phi_{sA} = 0.20$ (− −); $\phi_{sB} = 0.49$ (···).

PC there is a 25% decrease relative to l_{KB}. A similar procedure is performed this time with Brekner equation to describe the effective T_g's as ϕ_B varies. The TSDC results were fitted assuming that the dependence of $T_{gB}^{eff}(\phi)$ and $T_{gA}^{eff}(\phi)$ could also be described with the previously determined k_1 and k_2 parameters. The adjusted self-concentrations were now found to be $\phi_{sA} = 0.20$ and $\phi_{sB} = 0.49$. $T_{gA}^{eff}(\phi)$ and $T_{gB}^{eff}(\phi)$ variation calculated with these fitted effective concentrations are plotted in Figure 10. The adjusted value obtained for ϕ_{sA} is lower than that calculated with the Kuhn segment length of PCL. The large increase of ϕ_{sB}, 0.05 vs 0.49, is necessary to adjust the variation of the PC $T_{gB}^{eff}(\phi)$. Quantitative agreement in the description of the TSDC effective glass transitions for both components is now reached, as seen in Figure 10. The characteristic lengths calculated with these self-concentration values are $l_{cPCL} = 8.2$ Å and $l_{cPC} = 8.6$ Å. He et al.[14] have found that using the measured blend T_g's does not improve the fit quality and that the fit parameters obtained with the Fox equation are more consistent with the predicted ones. In our case both fittings are satisfactory; however, the characteristic lengths found in our second attempt (Brekner equation) might seem more consistent. The PC characteristic length being shorter than the PC Kuhn's length by using Brekner equation might be interpreted as the result of the loss of PC chains rigidity associated with the presence of PCL chains which plasticizes the PC. Additionally, the slight increase of l_{cA} might be indicative of the reciprocal effect in PCL as the cooperative mobility occurs in a glassy PC matrix.

Figure 11 shows results of dynamic mechanical measurements performed on the as-extruded ribbons in tensile mode. The values of the loss modulus E'' are plotted as a function of temperature. The data are consistent with the TSDC results presented above as the blends exhibit very broad peaks associated with the glass transition that for some composition are clearly bimodal. Therefore, a correspondence with the TSDC traces plotted in Figure 7 can be seen. In view of the lower resolution of the DMA the α relaxation mechanical modes are not as well-defined as those determined by TSDC; nevertheless, they are qualita-

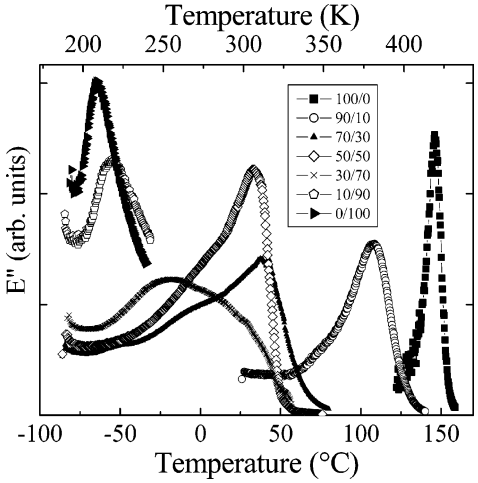

Figure 11. Variation of E'' as a function of temperature obtained by DMA testing on extruded PC/PCL blends.

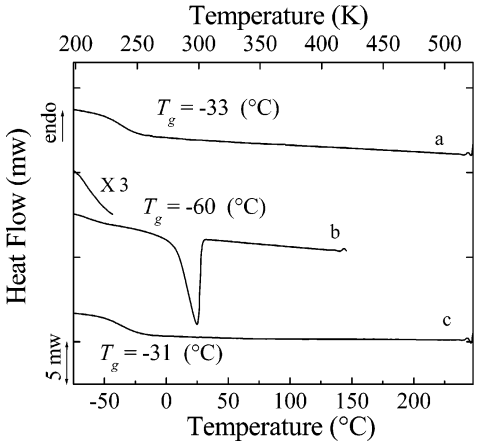

Figure 12. DSC cooling scans (20 °C/min) of 50/50 PC/PCL samples. Plot a is the standard cooling scan of the sample (similar thermal history to Figure 2). Plot b is a cooling run after annealing at 150 °C for 60 min. Plot c is the cooling run of the same sample after it was heated to 250 °C for 3 min.

tively similar, and the peak E'' values shift to higher temperatures as the PC content in the blends increases as expected.

In summary, the TSDC, DSC, and DMA results agree with the Lodge−McLeish model for these miscible blends where the PC component has been found to be 100% amorphous. In our previous work[9] on this same system the blends were found to be partially miscible with broad TSDC relaxations when the PC crystallinity was very low (quenched samples). On the contrary, when significant PC crystallinity degrees were found, as in the annealed samples, the phases were segregated as observed in the TSDC runs.

To verify this relationship between PC crystallinity and blend miscibility, isothermal PC crystallization experiments on the initially homogeneous blends were performed. Evidence of phase separation after PC crystallization was obtained by analyzing the thermal behavior of the blends after the PC component was isothermally crystallized at 130, 150, and 200 °C for 60 min. Figure 12 shows an example of the experiments performed to study the phase segregation induced in the blends by PC isothermal crystallization. Curve a of Figure 12 shows the standard cooling scan that is obtained when the 50/50 PC/PCL blend is cooled from the melt. Here the blend is miscible in the melt because

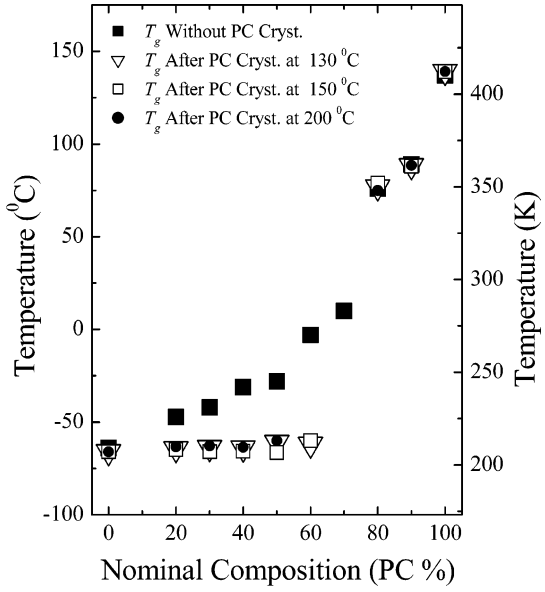

Figure 13. Values of T_g obtained by DSC cooling runs. The filled symbols correspond to T_g values obtained during standard DSC cooling runs (like those performed in Figure 2), and the other values were obtained after 60 min isothermal annealing treatments at the indicated temperatures.

during cooling only the bulk T_g is observed at −33 °C. However, if the PC component is thermally treated by heating the sample to 150 °C and performing an isothermal crystallization at this temperature for 60 min, the homogeneous blend can phase segregate during the PC crystallization process. This phase segregation phenomenon is reflected in Figure 12, curve b, where a cooling run from 150 °C (just after the PC isothermal crystallization step was performed) shows that the PCL component can now crystallize during cooling. Additionally, a T_g at around −60 °C is obtained, a very close value to the glass transition of neat PCL.

If the PC crystallization induces phase separation, and PC/PCL blends are supposed to be miscible in the amorphous phase, we would expect that melting the samples after PC crystallization would cause remixing if the melting temperature chosen is within the one phase region of the phase diagram (possibly below the lower critical solution temperature, LCST, that has been reported for this system[4−7]). Remixing was promoted by heating the sample to 250 °C and annealing at that temperature for 3 min. Curve c of Figure 12 shows the cooling DSC scan after the melting treatment was performed; a behavior similar to that of Figure 12, curve a, was obtained, evidencing miscibility once more.

A similar phase separation behavior was observed for blends containing 60% PC or less after PC was isothermally crystallized. The results are summarized in Figure 13. The T_g values obtained were similar to neat PCL T_g values (around −64 °C). This demonstrates that phase segregation can be induced by PC crystallization in blends containing up to 60% PC. For compositions equal to or higher than 80% no change on T_g values were observed. In addition, no endothermic jumps corresponding to T_g were detected for the 70/30 blend. It is possible that the transition could be masked by the PCL crystallization signal.

The T_g of the PC rich phase was not detected in any of the phase-segregated samples, a fact that may be related to rigid amorphous phase formation.[20]

4. Conclusions

In this study we have shown that PC/PCL blends, whose miscibility has deserved attention in recent literature, are miscible only when the PC component does not crystallize. In a previous study partial miscibility was found in samples where the PC showed a weak presence of crystals; also, in the case of slow cooled samples where the PC crystallinity degree reached 20%, the blends were not miscible as probed at different scales by TSDC, DSC, spherulitic growth, and transmission electron micrographs.[9] The samples used here were the extruded ribbons, air-cooled as they left the die, without any additional thermal treatment. In this condition we present the following evidence for the characteristics of the miscible mixture:

1. The blend is 100% amorphous until a 60/40 composition is reached. For PCL richer blends the poly(ϵ-caprolactone) crystallizes. No trace of development of PC crystallites is observed by WAXS at room temperature.

2. The blends are found to be homogeneous in the bulk with a single calorimetric T_g, intermediate between the T_g of the two neat components. The compositional variation of this bulk T_g cannot be precisely described by the Fox equation, but it can be successfully adjusted to Brekner's cubic expression.

3. For some compositions, PC and PCL could crystallize during cooling from the melt and/or during the heating DSC scan as shown by the melting endotherms in the DSC runs. Many factors can trigger the nucleation and further crystallization accompanied by the phase segregation when the PC crystallizes. Phase segregation is favored when PC is isothermally crystallized, but the homogeneity of the amorphous phase is restored if the PC crystalline phase is melted at high temperatures, but below the LCST of the blend.

4. The calorimetric glass transition observed by DSC is also broadened in the blends as compared to the homopolymers. The TSDC spectra for the blends do not show two sharp peaks at temperatures close to that of the homopolymers. Instead, one observes the existence of two different dynamics at intermediate temperatures evidenced by a composite α relaxation made of a sharp peak and a broader one. The Lodge−McLeish self-concentration model is applied to these two effective glass transition temperatures determined from TSDC and a qualitative agreement is found.

5. The agreement is significantly improved if the Kuhn length is not imposed as the length scale for the PC, as this high value leads to a very small self-concentration (0.05) for PC due to the chain rigidity. The higher self-concentration (shorter characteristic length) resulting from the best fit of the compositional variation of T_g^{eff} might be an indication of the loss of rigidity of the PC chains in the presence of PCL. PCL being a macromolecular plasticizer, it imparts enough mobility to PC chains so as to induce a reduction in the crystallization times. This result could be related to the enhancement of the local mobilities in the rich PCL blends observed by TSDC which was tentatively attributed to the loss of the rigid amorphous phase present in the rich PC blends.

6. Let us now try to answer in our case of blends made of polar and crystallizable components, the question posed by Kant et al.:[28] What length scales control the dynamics of miscible polymer blends? We found here that the relevant length is on the order of the Kuhn length for both components without the need to include any concentration or temperature dependence. In the case of the lower T_g component the size scale of cooperative motion around the effective T_g is somewhat larger (17%) than the Kuhn length possibly due to the constrains imposed by the PC neighboring chains. For the higher T_g component the characteristic length is lower than the Kuhn length of neat PC, but it still appears to be composition and temperature independent as a single self-concentration value can adjust the experimental points. The smaller cooperative volume found for PC in the miscible blend might be a consequence of the presence of the more flexible PCL chains acting as a molecular plasticizer.

Acknowledgment. We are indebted to FONACIT (Project G97000594) for partial funding of this project. D.H. acknowledges her Research Fellowship from Universidad Simón Bolívar.

References and Notes

(1) Varnell, D. F.; Runt, J. P.; Coleman, M. M. *Macromolecules* **1981**, *14*, 1350.
(2) Cruz, C. A.; Paul, D. R.; Barlow, J. W. *J. Appl. Polym. Sci.* **1979**, *23*, 589.
(3) Jonza, J. M.; Porter, R. S. *Macromolecules* **1986**, *19*, 1946.
(4) Cheung, Y. W.; Stein, R. S.; Wignall, G. D.; Yang, H. E. *Macromolecules* **1993**, *26*, 5365.
(5) Cheung, Y. W.; Stein, R. S. *Macromolecules* **1994**, *27*, 2512.
(6) Cheung, Y. W.; Stein, R. S.; Lin, J. S.; Wignall, G. D. *Macromolecules* **1994**, *27*, 2520.
(7) Cheung, Y. W.; Stein, R. S. *Macromolecules* **1994**, *27*, 3589.
(8) Balsamo, V.; Calzadilla, N.; Mora, G.; Müller, A. J. *J. Polym. Sci., Part B: Polym. Phys.* **2001**, *39*, 771.
(9) Hernandez, M. C.; Laredo, E.; Bello, A.; Carrizales, P.; Marcano, M.; Balsamo, V.; Grimau, M.; Müller, A. J. *Macromolecules* **2002**, *35*, 7301.
(10) Katana, G.; Fischer, E. W.; Hack, T. H.; Abetz, V.; Kremer, F. *Macromolecules* **1995**, *28*, 2714.
(11) Chung, G. C.; Kornfield J. A.; Smith, S. D. *Macromolecules* **1994**, *27*, 964.
(12) Kamath, S.; Colby, R. H.; Kumar, S.; Karatasos, K.; Floudas, G.; Fytas, G.; Roovers, J. E. L. *J. Chem. Phys.* **1999**, *111*, 6121.
(13) Lodge, T. P.; McLeish, T. C. B. *Macromolecules* **2000**, *33*, 5278.
(14) He, Y.; Lutz, T. R.; Ediger, M. D. *J. Chem. Phys.* **2003**, *119*, 9956.
(15) Leroy, E.; Alegría, A.; Colmenero, J. *Macromolecules* **2002**, *35*, 5587.
(16) Brekner, M. J.; Schneider, H. A.; Cantow, H. J. *Polymer* **1988**, *29*, 78.
(17) Haley, J. C.; Lodge, T. P.; He, Y.; Ediger, M. D.; von Meerwall, E. D.; Mijovic, J. *Macromolecules* **2003**, *36*, 6142.
(18) Hu, H.; Dorset, D. L. *Macromolecules* **1990**, *29*, 4604.
(19) Laredo, E.; Grimau, M.; Barriola, P.; Bello, A.; Müller, A. J. *Polymer*, in press.
(20) Laredo, E.; Grimau, M.; Müller, A. J.; Bello, A.; Suarez, N. *J. Polym. Sci., Polym. Phys*. **1996**, *34*, 2863.
(21) Grimau, M.; Laredo, E.; Perez, Y. M. C.; Bello, A. *J. Chem. Phys.* **2001**, *114*, 6417.
(22) Katana, G.; Kremer, F.; Fischer, E. W.; Plaetschke, R. *Macromolecules* **1993**, *26*, 3075.
(23) Zhang, S.; Runt, J. *J. Polym. Sci., Part B: Polym. Phys.* **2004**, *42*, 3405.
(24) Huang, Y; Xu, Z.; Huang, Y.; Ma, D.; Yang, J.; Mays, J. W. *Int. J. Polym. Anal. Charact.* **2003**, *8,* 373.
(25) Jones, A. A.; Stockmayer, W. H.; Molinari, R. J. *J. Polym. Sci., Polym. Symp.* **1976**, *54*, 227.
(26) Fetters L. J.; Lohse, D. J.; Richter, D.; Witten, T. A.; Zirkel, A. *Macromolecules* **1994**, *27*, 4639.
(27) Chung, G.-C.; Kornfield, J. A.; Smith, S. D. *Macromolecules* **1994**, *27*, 5729.
(28) Kant, R.; Kumar, S.; Colby, R. *Macromolecules* **2003**, *36*, 10087.

MA050481C